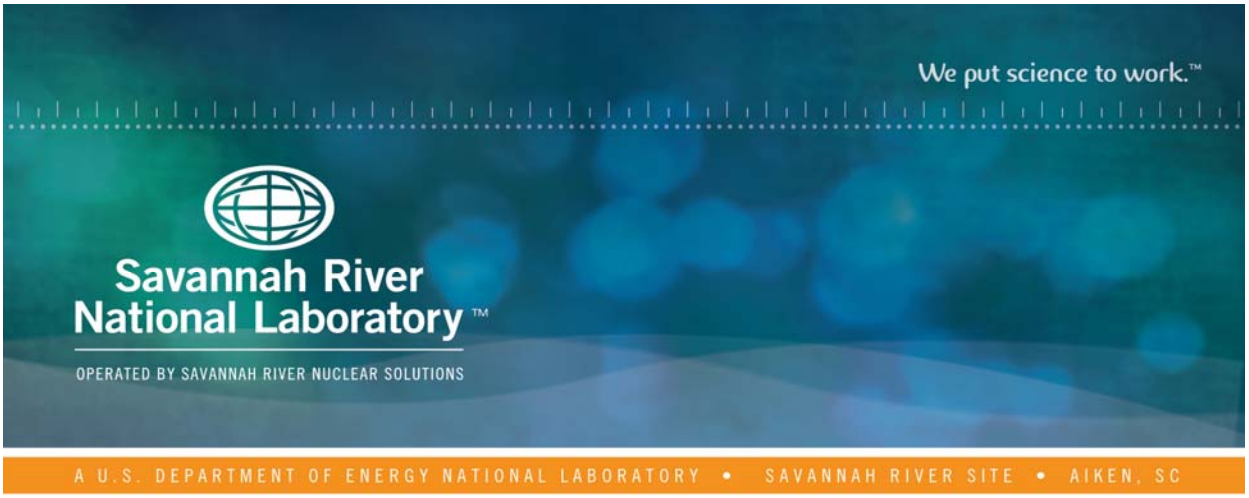

High-Temperature Oxidation of Stainless Steel for Fuel Cladding Removal

T. C. Shehee

R. A. Pierce

September 2014

SRNL-STI-2014-00432, Revision 0

DISCLAIMER

Printed in the United States of America

Prepared for
U.S. Department of Energy

SRNL-STI-2014-00432
Revision 0

Keywords: *decladding, stainless steel, induction heating*

Retention: *Permanent*

High-Temperature Oxidation of Stainless Steel for Fuel Cladding Removal

T. C. Shehee
R. A. Pierce

September 2014

Prepared for the U.S. Department of Energy under contract number DE-AC09-08SR22470.

Savannah River National Laboratory™
OPERATED BY SAVANNAH RIVER NUCLEAR SOLUTIONS

REVIEWS AND APPROVALS

AUTHORS:

_____

T. C. Shehee, Separation & Actinide Science Date

_____

R. A. Pierce, Separation & Actinide Science Date

TECHNICAL REVIEW:

_____

M. C. Thompson, Separation & Actinide Science Date

APPROVAL:

_____

T. B. Brown, Manager Date
Separation & Actinide Science

_____

S. L. Marra, Manager Date
Environmental & Chemical Process Technology Research Programs

EXECUTIVE SUMMARY

The Savannah River National Laboratory (SRNL) has been asked to explore alternate methods for decladding spent nuclear fuel. Of particular interest is the processing of stainless steel and zirconium clad fuels. However, the processing of clad fuel is bound by significant constraints associated with handling spent nuclear fuel in remote-handled environments. Several methods have been proposed for processing spent fuel using aggressive chemical, thermal, or mechanical methods. The most-common method used by industry is mechanical chop-leach or laser chop-leach where the fuel is cut into nominal one-inch segments and then the uranium in the fuel tubes is leached out of the segmented tubes using nitric acid. It is the assessment of Savannah River Site (SRS) subject matter experts that versions of chop-leach are prohibitively expensive for application at SRS.

The literature suggests another approach that would meet many of the characteristics of an ideal process. Fuel rods were perforated at a spacing of about one inch. After the perforations were complete, the fuel tubes were heated in air. As a result of heating in air, the fuel meat in the fuel tubes reacted with air, expanded, ruptured the stainless steel cladding at the perforations, and exposed the fuel meat for dissolution. However, that approach would require a method for perforating each individual fuel rod.

If the cladding could be weakened by an alternative method, perhaps the fuel rods would rupture and expose the fuel meat. One possible approach is high-temperature oxidation with air or steam. Under such conditions, the oxidized stainless steel may be brittle and friable enough to rupture when the fuel meat inside of the cladding expands. The results of these scoping studies indicate that it may be possible to breach stainless steel clad fuels and access the fuel meat in a similar manner.

Testing with 304L stainless steel coupons and tubes in a muffle furnace at temperatures near the melting point of 304L has shown that 304L tubing oxidizes readily to a brittle material. When 304L tubing is passed through an induction field to produce similar temperatures in the tube, the damage to the tube occurs faster and is more extensive than observed when heating the materials in a muffle furnace.

Experiments using tubes packed with Fe, V, and Ta metal powders showed that if the material inside the tube expands while the tube is made brittle through oxidation, cracking and perforation of the tube will occur along the length of the tube. The extent of damage was dependent upon metal powder used for testing. It is not known if any of the packing materials tested accurately represent the effect of UO_2 inside stainless steel tubes expanding as it is oxidized. The next stage of testing should consider the oxidation of an unirradiated fuel rod in an induction field.

TABLE OF CONTENTS

LIST OF TABLES

LIST OF FIGURES

LIST OF ABBREVIATIONS

psi	pounds per square inch
SRNL	Savannah River National Laboratory
SRS	Savannah River Site
XRD	X-ray Diffraction

1.0 Introduction

The Savannah River National Laboratory (SRNL) has been asked to explore alternate methods for decladding spent nuclear fuel. Of particular interest is the processing of stainless steel and zirconium clad fuels. However, the processing of clad fuel is bound by significant constraints associated with handling spent nuclear fuel in remote-handled environments. The ideal process for the Savannah River Site (SRS) would have the following characteristics.

1) Compatible with SRS Canyon operations
2) Simple process equipment concepts
3) Limited equipment and fuel handling
4) Suitable for various fuel bundle designs
5) Does not require fuel bundle disassembly
6) Little or no impact to the liquid waste system
7) Based on known technical concepts
8) Relatively benign process conditions

2.0 Background

Several methods have been proposed for processing spent fuel using aggressive chemical, thermal, or mechanical methods.[1] The most-common method used by industry is mechanical chop-leach[2] or laser chop-leach[3] where the fuel is cut into nominal one-inch segments and then the uranium in the fuel tubes is leached out of the segmented tubes using nitric acid. It is the assessment of SRS subject matter experts that versions of chop-leach are prohibitively expensive for application at SRS.[4]

Chemical decladding approaches have involved the use of either sulfuric acid or hydrochloric. In the large quantities required, both acids are incompatible with SRS waste streams.[5][6] Zirconium-clad fuels have been processed using solutions with high fluoride concentrations.[7] Reactive gases at elevated temperatures, such as HF or SF_6, have also been proposed but both would pose large off gas and waste handling issues.

The literature suggests another approach that would meet many of the characteristics of an ideal process.[8] In the 1960s, fuel rods were perforated at a spacing of about one inch. After the perforations were complete, the fuel tubes were heated in air. As a result of heating in air, the UO_2 in the fuel tubes reacted with air, expanded ~30% (theoretical), ruptured the stainless steel cladding at the perforations, and exposed the fuel meat for dissolution. While attractive, if it is necessary to process the fuel without disassembling the fuel bundles, the perforation step cannot occur.

If the cladding could be weakened by an alternative method, perhaps the fuel rods would rupture and expose the fuel meat. One possible approach is high-temperature oxidation with air or steam.[9][10][11] Several studies associated with fuel failure during accident scenarios show that stainless steel can be effectively oxidized in steam at 1200-1375 °C and in air at 1360-1385 °C. Under such conditions, the oxidized stainless steel may be brittle and friable enough to rupture when the UO_2 inside the cladding expands upon conversion to U_3O_8.

3.0 Experimental Procedures

3.1 Coupon Studies in a Muffle Furnace

The first stage of studies was completed using 304L stainless steel coupons and tubing segments heated in a muffle furnace. Seven experiments were completed with rectangular coupons and two with tubing

segments. In each case, the initial mass and thickness of the samples were recorded; the mass of an alumina (Al_2O_3) crucible was also recorded. The sample was then placed into an alumina crucible and introduced to the furnace. The furnace and sample were heated to a pre-determined temperature for a specified amount of time. At the completion of the heating cycle, the sample was cooled to room temperature, weighed, visual observations were conducted, and some samples were analyzed using X-ray Diffraction (XRD). A list of samples and test conditions is provided in Table 3-1.

Table 3-1. Samples and Test Conditions for Oxidation of 304L Coupons and Tube Segments

Test	Sample Type	Initial Mass (g)	Thickness (mm)	Furnace Temp (°C)	Time at Temp (min)	XRD?
1	Coupon	4.7402	1.16	1350	15	No
2	Coupon	4.5274	1.16	1350	30	Yes
3	Coupon	4.5499	1.16	1350	60	No
4	Coupon	4.5448	1.16	1375	15	No
5	Coupon	4.6852	1.16	1375	30	Yes
6	Coupon	4.4813	1.16	1375	60	No
7	Coupon	4.5475	1.16	1400	15	Yes
8	Tube Segment	9.0595	0.91	1375	60	Yes
9	Tube Segment	8.8677	0.91	1385	60	Yes

Subsequently, stainless steel tube segments were packed with fines of iron (Fe) metal, tantalum (Ta) metal, and vanadium (V) metal to identify a metal that would produce expansion due to air oxidation. The Fe powder was 99% (metals basis), -20 mesh from Alfa Aesar. The V powder was 99.5% (metals basis), ~325 mesh from Alfa Aesar. The Ta powder was 99.98% (metals basis), ~100 mesh from Alfa Aesar. The tube segments were 304L stainless steel measuring 10.5 mm outside diameter, 1.02 mm wall thickness, and 68-77 mm long.

The tubes were packed using a hydraulic press and a pellet die that made use of a bottom section from a commercially available pellet die, a 4” body machined from stainless steel, and a packing rod made from a cut off drill bit. The die set was fabricated by the SRNL Machine Shop. The base and body of the die were assembled by placing the body on top of the base. The inside of the die body and the outside of the tube were coated with a 5% steric acid / alcohol solution. The steric acid acts as a high pressure lubricant to minimize galling between the sample tube and the die body. The sample tube was inserted into the die body and filled to ~1 cm from the top of the tube. The packing rod was inserted into the die body and the entire assembly was placed on a bench top hydraulic press. The packing rod OD was slightly smaller than the ID of the tube. Once placed in the press, pressure was increased slowly with several releases of the pressure to ensure the packing rod was lined up correctly with the body to minimize galling. Tubes were pressed to a maximum pressure of 4000 – 8000 pounds per square inch (psi). On completion of the packing, the tube was pressed out of the die body

Test conditions for the packed tubes are listed in Table 3-2. For the Fe metal powder, the tube was pressed to 4000 psi. The powder depth in the tube was ~40 mm. The Fe-packed tube was heated to 1375 °C in air in the muffle furnace for one hour, inspected, two additional hours, inspected, and a final two hours (total of five hours at temperature). For the V metal powder, the tube was pressed to 7000 psi. The powder depth in the tube was 30.3 mm. For the Ta metal powder, the tube was pressed to 8000 psi with a final powder depth of 11.5 mm. The V-packed and Ta-packed tubes were heated to 1375 °C in air for one hour, cooled, and inspected.

Table 3-2. Conditions for Oxidation of Packed Tube Segments in a Muffle Furnace

Test	Packing	Packing Pressure (psi)	Packing Depth (mm)	Furnace Temp (°C)	Time at Temp (min)
10	Fe metal	4000	~40	1375	300
11	V metal	7000	30.3	1375	60
12	Ta metal	8000	11.5	1375	60

3.2 Studies with Tubes in an Induction Field

A series of studies was conducted with 304L stainless steel tubing (12.6-12.7 mm outside diameter, 0.86-0.90 mm wall thickness, 72-75 mm long). Test variables included temperature, time at temperature, packed versus unpacked tubes, packing material, and presence or absence of steam. A picture of the equipment for oxidation of tube segments is shown in Figure 3-1. The induction field is generated with an Ameritherm HotShot 3.5 induction heater – the unit is capable of 3.5 kW. The coil inside diameter is 32 mm and the coil height is 17 mm. The induction heater was cooled with a Neslab Thermoflex 900 recirculating chiller set at 25 °C.

Tests were performed with both empty and packed 304L tubes and empty Alloy 625 tubes. The 304L tubes were packed with powders of Fe metal and Ta metal. The Fe powder was 99% (metals basis), -20 mesh, from Alfa Aesar. The Ta powder was 99.9% (metals basis), -22 mesh, from Alfa Aesar. The tubes were packed in the manner described in Section 3.1. The tubes were oxidized while passing the packed tube through the induction field.

The first tests were completed with stationary samples of empty 304L tubes. The 304L tube sample was loaded into the sample holder and held in place with two set screws. The sample holder was secured in the sample advance mechanism with two other set screws. The sample is positioned with sample centered in the opening of the induction coil and the bottom of the sample ~0.5 cm below the bottom of the induction coil. The induction coil was then turned on at a specified amperage for a specific amount of time. At the conclusion of the test, the power was turned off and the sample cooled to ambient temperature for visual inspection.

During this stage of testing, the temperature at the center of the coil as a function of amperage was measured. This was necessary because testing with packed tubes made it impossible to have a thermocouple in the center of the field during testing. The amperage-temperature profile was measured for both an open tube and a tube with a sealed end on the side in the induction field; both tubes were empty. Temperature with the closed tube was measured using a Type K thermocouple attached to an Omega HH22 thermocouple reader. The temperature for the open tube was measured using a Type S thermocouple attached to a millivolt (Fluke Model 177) reader. The millivolt readings were converted to temperature using standard tables.[12] These data are listed in Table 3-3 and plotted in Figure 3-2. These data were used as a guide for selection of test settings. For the selected amperage range used during testing, there was little difference in the temperature of the open and closed tubes (based on extrapolation of the closed-tube data).

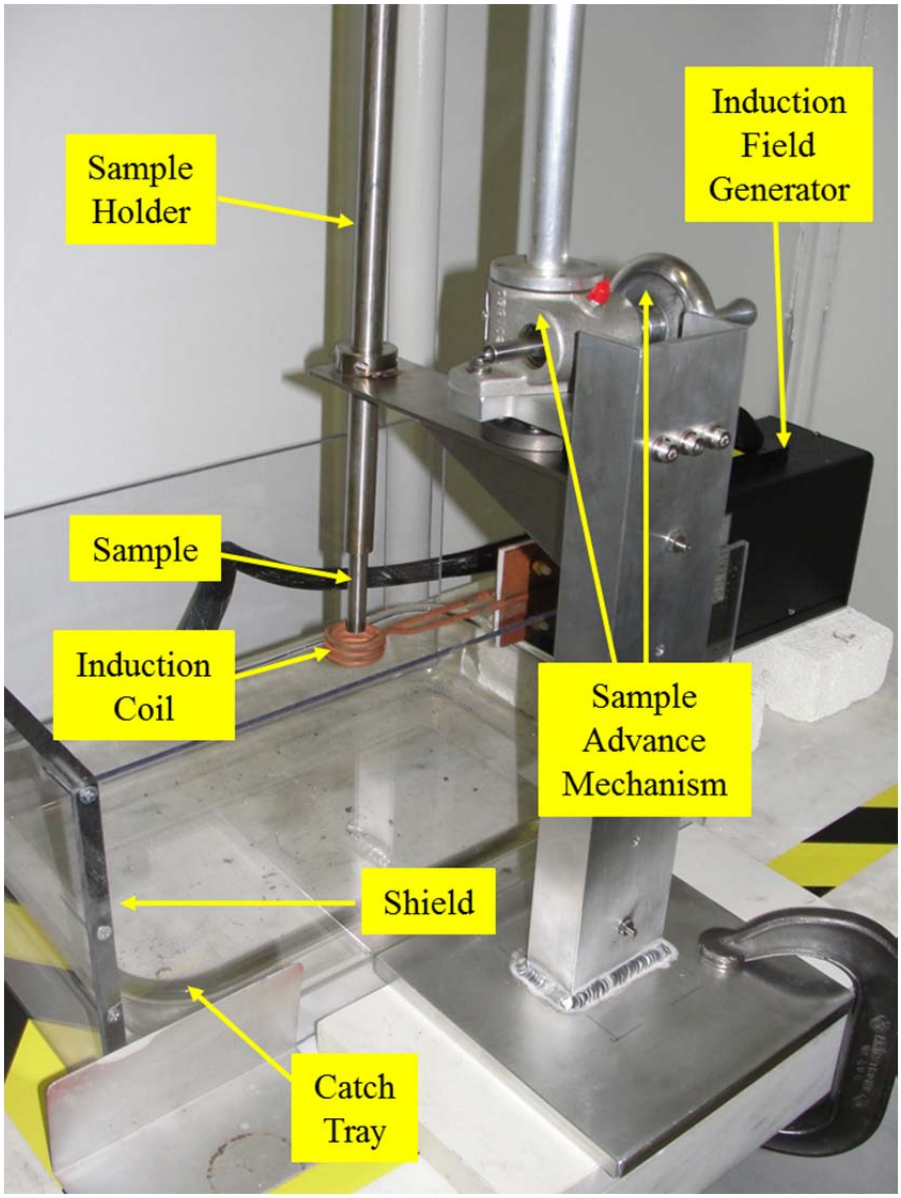

Figure 3-1. Equipment for Oxidation of Samples in an Induction Field

Table 3-3. Amperage-Temperature Data for Open and Closed Tubes

Closed Tube Power (amps)	Closed Tube Temp (°C)	Open Tube Power (amps)	Open Tube Reading (mV)	Open Tube Temp (°C)
0	23	0	0	23
49.4	320	49.4	-1.4	193
75.2	545	75.2	-3.4	398
101.0	730	101	-5.1	557
124.7	868	124.7	-6.6	688
150.5	1000	150.5	-8.3	828
174.1	1080	174.1	-9.8	945
199.9	1176	199.9	-11.4	1067
219.3	1238	219.3	-12.5	1147
225.7	1260	225.7	-12.8	1169
		249.4	-14.1	1262
		275.2	-16.3	1418

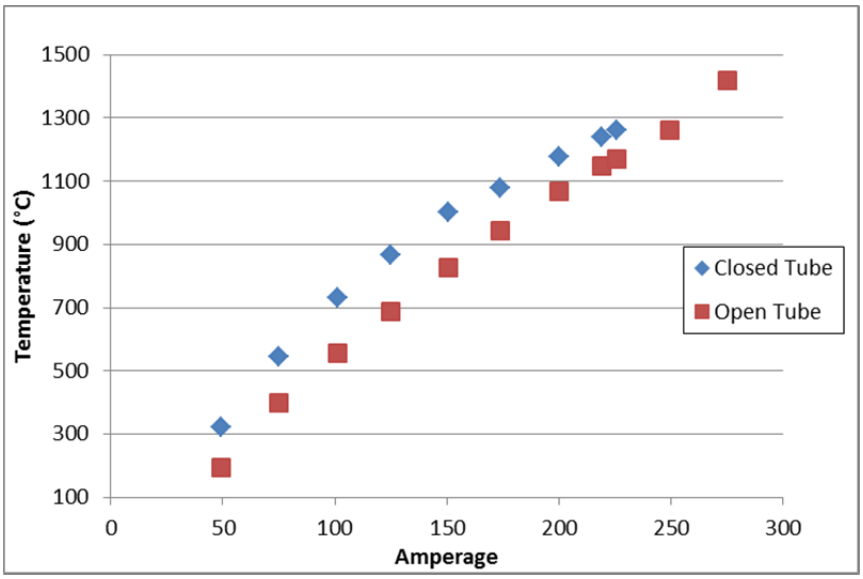

Figure 3-2. Amperage-Temperature Profiles for Open and Closed Tubes

In the second series of tests, the tubes were advanced through the induction field at a specified rate. Each tube was loaded into the sample holder and held in place with two set screws. The sample holder was secured in the sample advance mechanism with two other set screws. The sample is positioned with the bottom of the sample even with the top of the induction coil and the sample centered in the opening of the induction coil. Power to the induction coil was provided and the system operated for 30 s prior to advancing the sample through the induction coil.

The sample was then advanced regularly after a specified amount of time. Each advance entailed turning the sample advance mechanism five turns at 0.63 mm/turn (or 3.15 mm/advance). Because it was determined that 60 turns were sufficient to put all of the packing material into the center of the induction field, a total of 55-75 turns were used in each test for a total advance distance of 34.65-47.25 mm. Test conditions are listed in Table 3-4. During Test D, a continuous mist of deionized water was provided at

the surface of the sample in the heated zone. This was accomplished through the use of a spray bottle with a mist setting.

Table 3-4. Conditions for Oxidation of Tube Segments in an Induction Field

Test	Packing	Packing Pressure (psi)	Packing Depth (mm)	Induction Amperage	Estimated Temp (°C)	Advance Interval (s)	Advance Distance (mm)
A*	Fe metal	8000	40.7	251.5	1350	15	47.25
B*	Fe metal	8000	44.5	251.5	1350	30	47.25
C*	Fe metal	8000	43.6	275.2	1425	15	47.25
D*†	Fe metal	8000	38.0	251.5	1350	15	40.95
E*	Fe metal	8000	37.1	275.2	1425	30	40.95
F*	Fe metal	8000	38.0	251.5	1350	45	40.95
G*	Ta metal	8000	25.8	251.5	1350	60	40.95
H*	Ta metal	8000	24.9	275.2	1425	60	40.95
I*	Ta metal	8000	25.8	275.2	1425	90	40.95
J#	Empty	---	---	251.5	1350	15	34.65
K#	Empty	---	---	251.5	1350	30	34.65

* 304L stainless steel, 12.6-12.7 mm outside diameter, 0.86-0.90 mm wall thickness
† Performed in steam environment by injecting a mist into the heated zone
# Alloy 625, 9.6 mm outside diameter, 0.95 mm wall thickness

4.0 Results and Discussion

4.1 Coupon Studies in a Muffle Furnace

Testing with coupons (Table 3-1) showed a distinct oxidation behavior as a function of time and temperature. The test conditions and mass-increase data are provided in Table 4-1. The temperature effect can be seen best in the change of mass and thickness for Tests 1, 2, and 3. Apart from the Test 6 sample, the % mass increase appears to plateau at 28-31%. The thickness increase plateau was 135-145%. A comparison of before and after samples for the coupons (Test 2) and tube segments (Test 9) is shown in Figure 4-1.

The samples were inspected and the coupons were subjected to flexing by hand. The samples from Tests 1, 2, 4, and 5 retained some measure of flexibility, although a significant layer of the material delaminated from the sample. Pictures of the sample and some delaminated material are shown in Figure 4-2. The coupons from Tests 6 and 7 fractured without flexing. The fractured samples from these two tests are presented in Figure 4-3. A close examination of the sample from Test 7 (Figure 4-3, bottom) shows a thin piece of residual metal sample. The samples from Tests 8 and 9 fractured readily without flexing and exhibited sample cross-sections comparable to that of Test 6 (Figure 4-3, top).

Table 4-1. Oxidation of 304L Stainless Steel Coupons and Tube Segments

Test	Sample Type	Temp (°C)	Time (min)	Initial Mass (g)	Final Mass (g)	% Mass Increase	Final Thickness (mm)	% Thickness Increase
1	Coupon*	1350	15	4.7404	5.5267	16.6	2.06	77.6
2	Coupon*	1350	30	4.5275	5.5922	23.5	2.15	85.3
3	Coupon*	1350	60	4.5498	5.9677	31.2	2.81	142.2
4	Coupon*	1375	15	4.5449	5.5131	21.3	2.24	93.1
5	Coupon*	1375	30	4.6852	5.9651	27.3	2.71	133.6
6	Coupon*	1375	60	4.4815	6.1728	37.7	3.23	178.4
7	Coupon*	1400	15	4.5472	5.9102	30.0	2.13	83.6
8	Tube#	1375	60	9.060	11.6200	28.3	2.18	139.6
9	Tube#	1385	60	8.8677	11.5111	29.8	2.23	145.1

* Coupon thicknesses were 1.16 mm
# Tube thicknesses were 0.91 mm

Figure 4-1. Comparison of Initial and Final Samples for Test 2 (left) and Test 9 (right)

Figure 4-2. Comparison of Delaminated Samples for Test 1 (left) and Test 4 (right)

The oxidation studies confirmed that at 1375-1385 °C, stainless steel coupons and tubing segments with material thicknesses about twice that of fuel cladding can be completely oxidized in 30-60 minutes. At 1400 °C, oxidation occurs within 15 min but some melting of the steel also occurs. Oxidation in air at 1350 °C in a muffle furnace is prohibitively slow, which is consistent with the data in the literature.[9]

Once oxidized, the oxidized tube samples were sufficiently brittle to fracture with a small amount of compressive force. It is not known if the sample will fracture in tension due to an expanding powder within the oxidized tube.

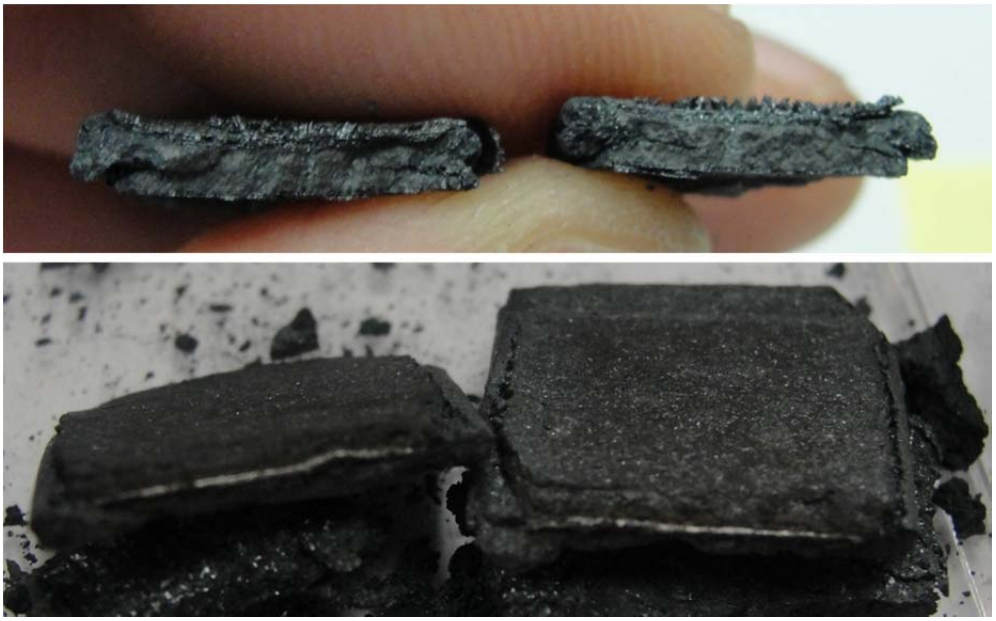

Figure 4-3. Fractured Samples for Test 6 (top) and Test 7 (bottom)

Samples from Tests 2, 5, 6, 7, 8, and 9 were analyzed by XRD. The data are provided in Table 4-2. XRD analyses of oxidized 304L identified chromite ($FeCr_2O_4$), hematite (Fe_2O_3), and wustite (FeO) as major phases in oxidized material with no detectable residual metal. Awaruite ($FeNi_3$) was observed as a minor phase in the samples from Tests 5 and 9. Although the sample from Test 8 fractured readily, the XRD still shows a significant fraction of iron present as metal. The result from Test 8 (at 1375 °C) is a contrast to the result from Test 9 (1385 °C), which shows no detectable unoxidized metal.

Table 4-2. XRD Data for Tests 2, 5, 7, 8, and 9

Test	Sample Type	Temperature (°C)	Time (min)	Major Crystalline Phases	Minor Crystalline Phases
2	Coupon	1350	30	$FeCr_2O_4$, Fe_2O_3	
5	Coupon	1375	30	$FeCr_2O_4$, Fe_2O_3	$FeNi_3$
7	Coupon	1400	15	$FeCr_2O_4$, Fe_2O_3	
8	Tube	1375	60	$FeCr_2O_4$, Fe, FeNi	Fe_2O_3, FeO
9	Tube	1385	60	$FeCr_2O_4$, FeO	Fe_2O_3, $FeNi_3$

Testing with 304L tubes packed with Fe, V, and Ta metal powders (Table 3-2) yielded different responses. Images of the tubes after oxidation in the muffle furnace at 1375 °C are provided for the tubes packed with Fe (Figure 4-4), V (Figure 4-5), and Ta (Figure 4-6). The side views of the Fe-packed tube exhibited increased embrittlement and cracking with increased times. In Figure 4-4, the packed Fe was sticking out of the end of the tube at the beginning of the experiment. As the test progressed, there appeared to be no growth of the packed material, either radially or axially, sticking from the tube.

The side views for V and Ta clearly show the material packing depths as evidenced by the increased tube diameter. The end views for V and Ta indicate that V did not oxidize in the same manner as Ta. The edge of the V and Ta were not analyzed, but the appearance of the V is that of metal and Ta is that of oxide. Because of the results, Fe (because of availability) and Ta (because of oxidation behavior) were selected for the testing of packed tubes passing through an induction field.

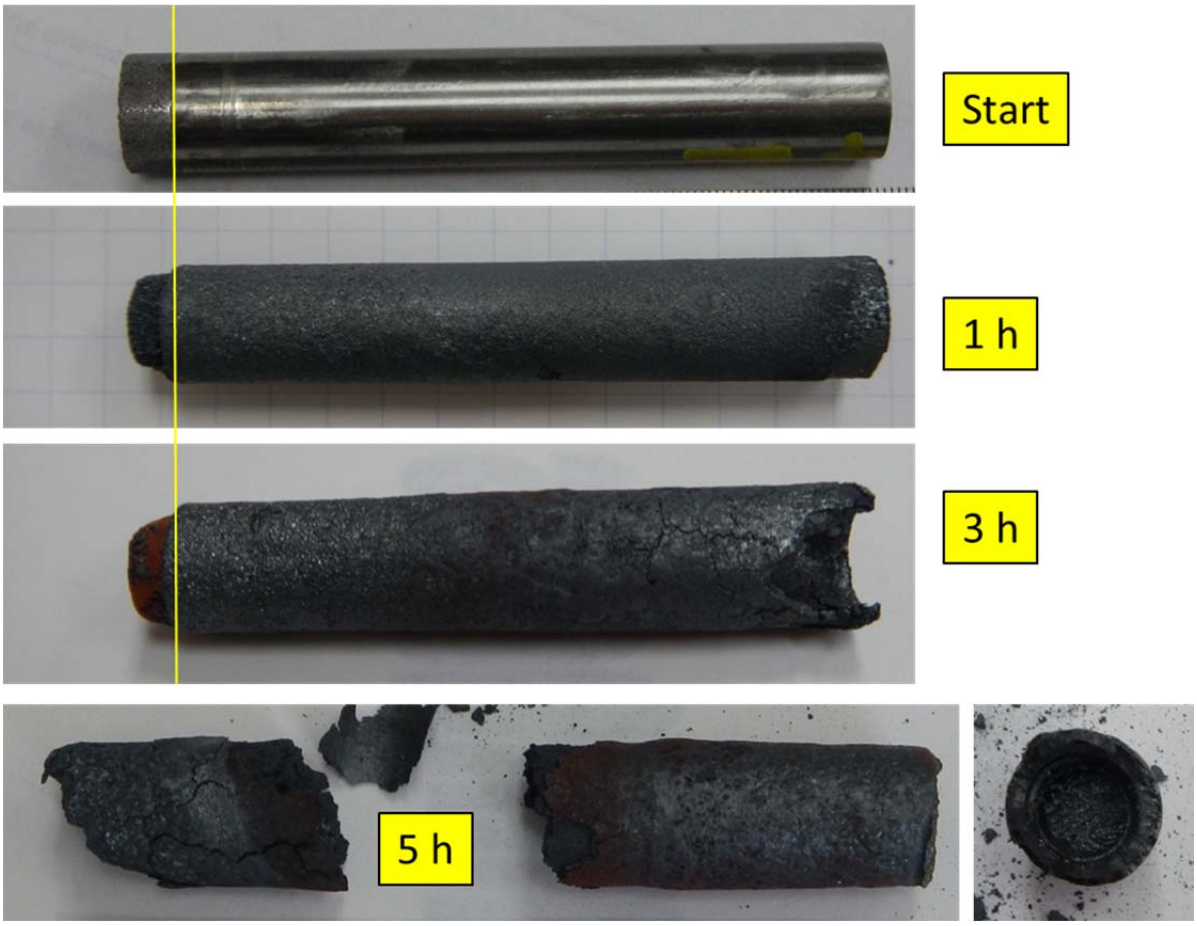

Figure 4-4. Tube Packed with Iron after Oxidation in Muffle Furnace at 1375 °C

Figure 4-5. Tube Packed with Vanadium after Oxidation in Muffle Furnace at 1375 °C

Figure 4-6. Tube Packed with Tantalum after Oxidation in Muffle Furnace at 1375 °C

4.2 Studies with Tubes in an Induction Field

A series of observations were made of each sample after heating in the induction field. Those observations are provided in Table 4-3. Stainless steel readily interacts with the induction field to produce rapid temperature increases in the tube. As discussed in Section 3.2, the actual temperature in the center of the tubes was not known. The temperatures can only be inferred from the data in Figure 3-2. The two test temperatures for the experiments listed in Table 4-3 were estimated at 1350 °C (251.5 amps) and 1425 °C (275.2 amps). The melting point of 304L stainless steels is ~1380 °C. Pictures of Fe-packed tubes are in Figure 4-7 and Figure 4-8. Pictures of Ta-packed tubes are presented in Figure 4-9. Figure 4-10 and Figure 4-11 show the empty Alloy 625 tube after heating in the induction field.

Table 4-3. Observations for Oxidation of Tube Segments in an Induction Field

Test	Packing	Induction Amperage	Advance Interval (s)	Observations
A*	Fe metal	251.5	15	Deep gouges are breaches in the tube wall
B*	Fe metal	251.5	30	Well-defined crack for length of metal powder
C*	Fe metal	275.2	15	Substantial damage. Difficult to distinguish between melted tube and melted powder inside
D*†	Fe metal	251.5	15	Well-defined crack near the edge of the tube; not as long of a crack as for Sample B
E*	Fe metal	275.2	30	Substantial damage. Difficult to distinguish between melted tube and melted powder inside
F*	Fe metal	251.5	45	Small crack at the edge; no other holes
G*	Ta metal	251.5	60	Cracking occurring where powder expansion occurs
H*	Ta metal	275.2	60	Significant damage plus cracking where powder expands
I*	Ta metal	275.2	90	Significant damage plus cracking where powder expands
J#	Empty	251.5	15	Significant wall damage; probing with a pointed object reveals significant weakness in the wall
K#	Empty	251.5	30	Less apparent damage than Sample J

* 304L stainless steel, 12.6-12.7 mm outside diameter, 0.86-0.90 mm wall thickness
† Performed in steam environment by injecting a mist into the heated zone
# Alloy 625, 9.6 mm outside diameter, 0.95 mm wall thickness

Testing with tubes packed with either Fe- or Ta-packed tubes shows a large difference between the appearances after processing at 251.5 amps and 275.2 amps (Figure 4-7). At 275.2 amps, it appears that the tubes are melting. It is difficult to tell from visual observation the extent of breaching through the tube wall because the melted tube interacts to some degree with the Fe metal powder (mp = 1535 °C).

At 251.5 amps, the bump-filled surface observed at 275.2 amps is replaced with a smooth surface with distinct cracks. The appearance of the cracks at 251.5 amps is depicted in Figure 4-8. The extent of cracking does not appear to be a function of dwell time, based on a comparison of the tubes from Tests A (15 s), B (30 s), and G (45 s). Tests A and B appear to have more visible damage than Test C. This may be attributable to variations in the tube material (e.g., wall thickness) or specific orientation within the induction field. The addition of a water mist (resulting in steam) in the heating area did not noticeably accelerate degradation of the tube, as was anticipated based on data in the literature.[8] Although different quantities of steam and longer dwell times may increase the effect of steam, the objective was for the presence of steam to significantly reduce the operating temperature for the same dwell times at the expense of a more-complicated off gas stream. Those benefits do not appear to be realized in the short dwell times being employed in the induction field.

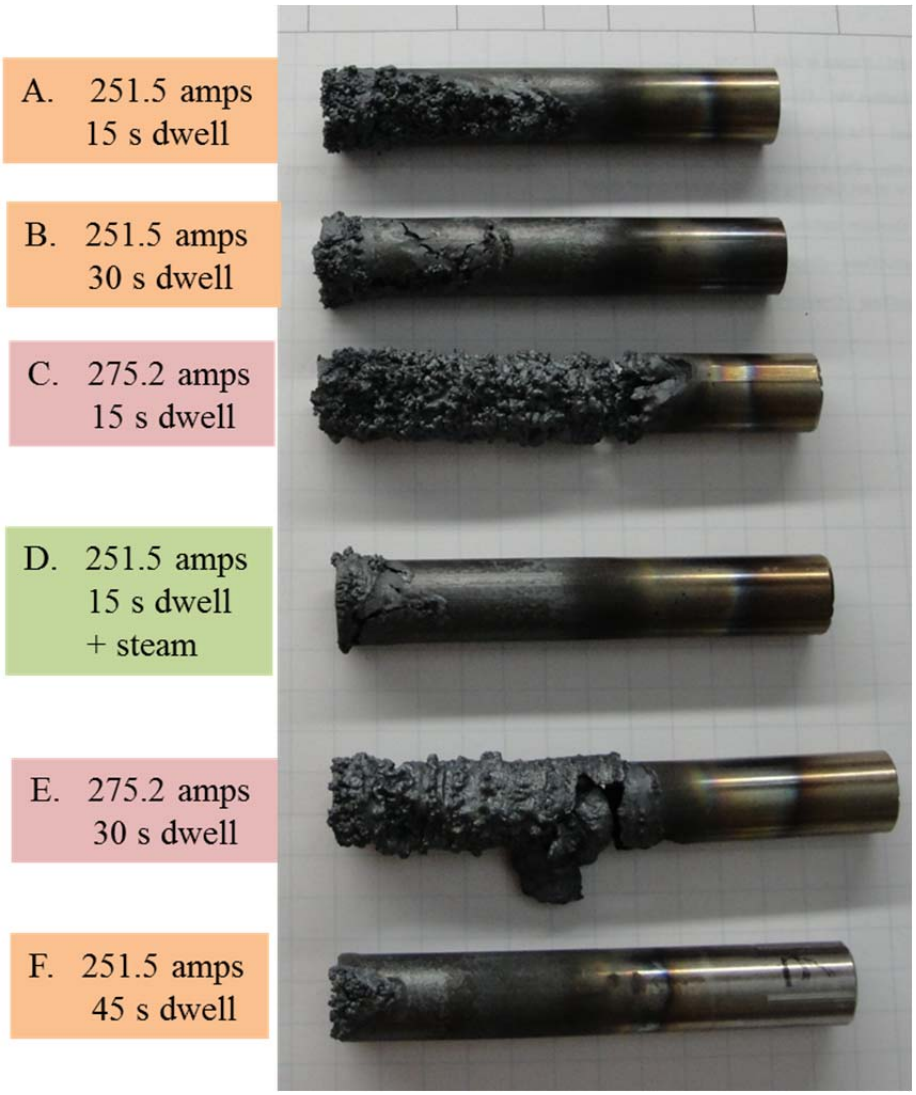

Figure 4-7. Tubes Packed with Iron after Oxidation in an Induction Field

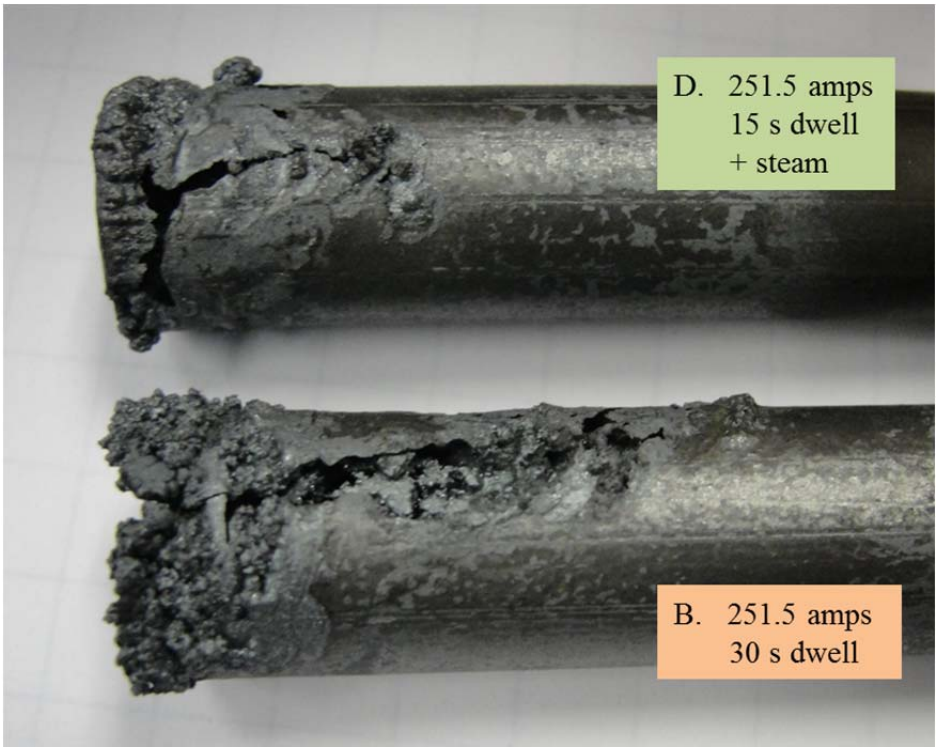

Figure 4-8. Comparison of Tubes B and D after Oxidation in an Induction Field

If the temperatures estimated in Table 3-4 are accurate, then significant damage is occurring at a temperature (1350 °C) that was not sufficiently high to produce significant damage in the muffle furnace samples. The difference between the Fe-packed tube at 1375 °C in the muffle furnace for 5 h (Figure 4-4) exhibits significantly less damage to the tubing than at 1350 °C in the induction field for less than 10 min (Figure 4-8). It is not known whether this can be attributed directly or indirectly to the induction field. It may also be attributable to interaction between the Fe metal powder inside the tube with the induction field.

Testing with Ta metal powder also resulted in cracking of the tubes (Figure 4-9), but the cracking was not as extensive at 251.5 amps. The overall damage at the higher power setting of 275.2 amps was not as extensive either. It should be noted that the large holes visible in Samples H and I occur above the space occupied by Ta metal powder.

It can be seen in Figure 4-9 that the Ta metal has been oxidized to tantalum oxide (TaO_2), which expands due to its lower density compared to that of the metal powder. Some of the expansion is out the bottom of the tube. Consequently, the Ta expansion does not produce as much cracking of the tube. The same expansion out the bottom of the tube was not observed for the Fe-packed tubes in the induction field (Figure 4-7).

Figure 4-9. Tubes Packed with Tantalum after Oxidation in an Induction Field

Two tests were completed with empty segments of Alloy 625 tubing at the request of the customer to determine if the oxidation method behaved similarly for nickel-based alloys. Pictures from those two tests are shown in Figure 4-10 and Figure 4-11. Both tubes show significant damage at 251.5 amps. When the tube from Test J was probed with a pointed file (Figure 4-11), it was observed that the wall in the damaged area was weak and was readily breached. It is not known if there were holes prior to the probing.

Figure 4-10. Empty Alloy 625 Tubes after Oxidation in an Induction Field

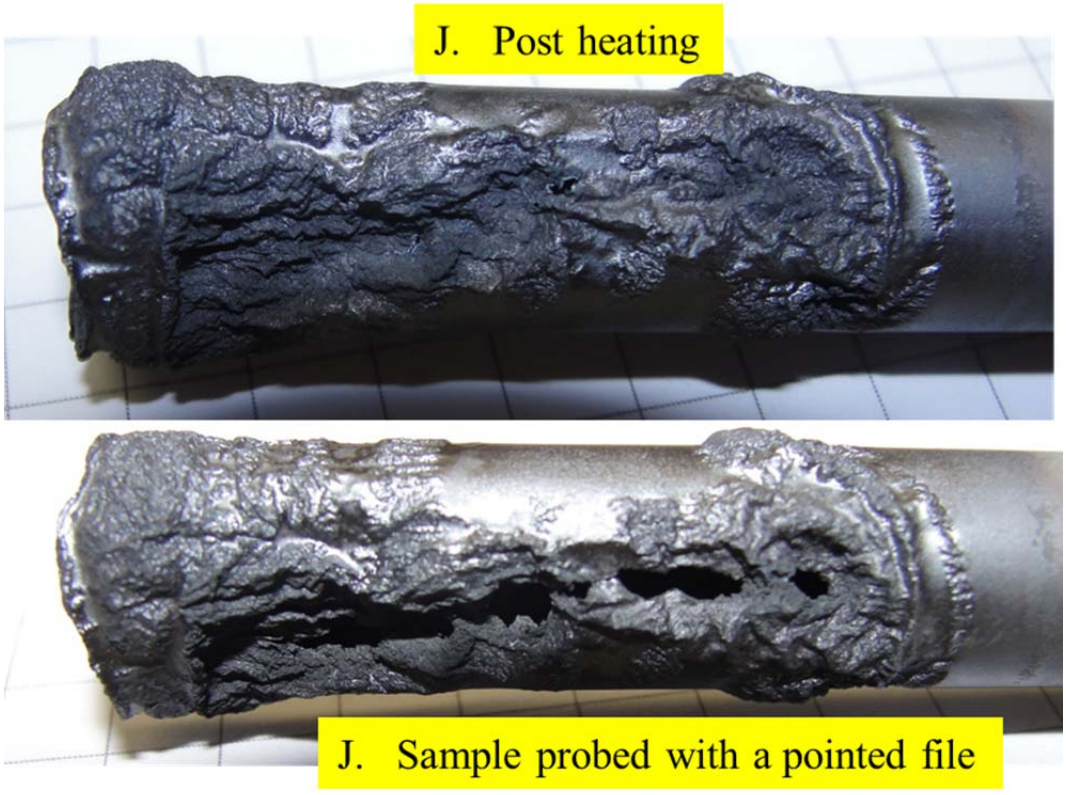

Figure 4-11. Empty Alloy 625 Tube after Oxidation in an Induction Field – Before Probing (top) and After Probing (bottom)

5.0 Conclusions

The results of these scoping studies indicate that it may be possible to breach stainless steel clad fuels and access the fuel meat in a manner similar to the AIROX process.[8] The approach taken involves oxidizing the tubing to make it brittle and crack, and then the UO_2 fuel meat inside the tube oxidizes and expands to split the tubing open and expose the fuel meat.

Testing with 304L stainless steel coupons and tubes at elevated temperatures (1350-1425 °C) has shown that 304L tubing oxidizes to a brittle material comprised mostly of chromite ($FeCr_2O_4$) and hematite (Fe_2O_3). When 304L tubing is passed through an induction field to produce similar temperatures in the tube, the damage to the tube occurs faster and is more extensive than observed when heating the materials in a muffle furnace. Similar behavior was observed for tubing made from nickel-based Alloy 625.

Experiments using tubes packed with Fe, V, and Ta metal powders showed that if the material inside the tube expands while the tube is made brittle through oxidation, cracking and perforation of the tube will occur along the length of the tube. The extent of cracking was dependent upon metal powder used for testing. It is not known if any of the materials tested accurately represent the effect of UO_2 inside stainless steel tubes expanding as it is oxidized to U_3O_8 (30% expansion).

For Fe-packed tubes, significant cracking occurred at ~1350 °C and melting of the tube was evident at ~1425 °C. The extent of tube cracking or damage did not appear to be a function of dwell time from 15-45 seconds. For Ta-packed tubes, minor cracking occurred at ~1350 °C with more extensive cracking and tube degradation at ~1425 °C; however, the tube appearance after testing is very different from that of the Fe-packed tubes at the same temperature. The presence of a water mist (which turns to steam) in the heating zone did not visibly change the magnitude of tube degradation.

6.0 Future Work

At the current stage of development, it is envisioned that the next stage of trials would involve work with an unirradiated fuel rod, preferably fabricated with natural or depleted uranium. The trials could be conducted in the SRNL Fab Lab. An unirradiated fuel rod would be fed slowly in air into an induction field to allow oxidation of the cladding. Testing would have to be conducted at varying power settings and feed rates.

Consideration should also be given to the length of the induction field. What would be the impact of a longer field? While it might accelerate the process, might it also have negative impacts? For example, if a rod were oxidized all at once, it could fracture first in the middle and fall into the bottom of a holding container. However, the broken pieces might also get lodged in the coil or damage the coil through contact of the cold coil with hot materials.

The first proposed approach is to gradually feed the tube into a heating zone so that oxidation of the metal is gradually up the tube and fracture of the tube occurs first at the bottom and then progresses up the tube. This approach may be necessary to produce behavior in the tube similar to that of chop-leach (i.e., fracturing in small segments to expose the fuel meat). Based on preliminary studies described, it is expected that the rod will retain its mechanical integrity and not form a series of small segments.

7.0 References

1. W. D. Bond, J. C. Mailen, and G. E. Michaels, "Evaluation of Methods for Decladding LWR Fuel for a Pyroprocessing-Based Reprocessing Plant", ORNL/TM-12104, January 1994.
2. G. F. Kessinger and M. C. Thompson, "Chop-Leach Dissolution of Commercial Reactor Fuel", *AIP Conference Proceedings*, **2003,** 673(1), 288.
3. P. D. Gupta, "Laser Applications in Indian Nuclear Power Programme", *Energy Procedia 00(2010)*, Elsevier Publishing, *www.sciencedirect.com*.
4. D. E. Eyler, "H Canyon Cold Crucible Induction Melter (CCIM) and Fuel Shear/Leach Estimates", SRNL-L0000-2012-00505-DEP, March 30, 2012.
5. R. E. Blanco, L. M. Ferris, and D. E. Ferguson, "Aqueous Processing of Thorium Fuels", ORNL-3219, February 1962.
6. B. C. Finney and B. A. Hannaford, "Sulfex Process: Engineering-Scale Semicontinuous Decladding of Unirradiated Stainless Steel-Clad UO_2 and UO_2-ThO_2", ORNL 3072, March 1961.
7. R. E. Blanco, L. M. Ferris, and C. D. Watson, "Preparation of Stainless Steel, Zirconium, and Graphite Clad and Base Reactor Fuels for Solvent Extraction", ORNL-TM-131, January 1962.
8. L. F. Grantham, R. G. Clark, R. C. Hoyt, and J. R. Miller, "AIROX Dry Pyrochemical Processing of Oxide Fuels", Actinide Separation, *ACS Symposium Series 117*, **1980,** 219-232.
9. J. T. Bittel, L. H. Sjodahl, and J. F. White, "Oxidation of 304L Stainless Steel by Steam and by Air", *Corrosion – NACE*, **1969,** 25(1), 7-14.
10. R. Guillamet, J. Lopitaux, B. Hannoyer, and M. Lenglet, "Oxidation of Stainless Steels (AISI 304 and 316) at High Temperature", *J. de Physique IV*, Colloque C9, **1993**, 3, 349-356.
11. T. Ishida, U. Harayama, and S. Yaguchi, "Oxidation of 304 Stainless Steel in High-Temperature Steam", *J. Nucl. Mat.*, **1986,** 140, 74-84.
12. "Revised Thermocouple Reference Tables, Type S", *www.omega.com/temperature/Z/pdf/z208-209.pdf* , September 22, 2014.

Distribution:

T. M. Adams, 773-41A
W. F. Bates, 703-H
T. B. Brown, 773-A
T. B. Calloway, 999-2W
S. D. Fink, 773-A
C. C. Herman, 773-A
D. T. Herman, 735-11A
D. T. Hobbs, 773-A
E. N. Hoffman, 999-W
S. L. Marra, 773-A
M. C. Thompson, 773-A
J. C. Marra, 999-2W
G. M. Maxted, 703-H
D. H. McGuire, 999-W
F. M. Pennebaker, 773-42A
R. A. Pierce, 773-A
T. C. Shehee, 773-A
R. M. Sprague, 773-A
J. R. Jackson, 703-46A
Records Administration (EDWS)